Limitations of Current Polarization for Lowering the Detection Limit of Potentiometric Polymeric Membrane Sensors

ARTICLE *in* ANALYTICAL CHEMISTRY · MAY 2009

Impact Factor: 5.64 · DOI: 10.1021/ac802588j · Source: PubMed

6 AUTHORS, INCLUDING:

Lajos Höfler
Budapest University of Technology and Econ…
16 PUBLICATIONS **226** CITATIONS
SEE PROFILE

Tamas Vigassy
Metrohm AG
17 PUBLICATIONS **591** CITATIONS
SEE PROFILE

Róbert E Gyurcsányi
Budapest University of Technology and Econ…
94 PUBLICATIONS **1,978** CITATIONS
SEE PROFILE

Eric Bakker
University of Geneva
291 PUBLICATIONS **13,796** CITATIONS
SEE PROFILE

Published in final edited form as:
Anal Chem. 2009 May 1; 81(9): 3592–3599. doi:10.1021/ac802588j.

Limitations of Current Polarization for Lowering the Detection Limit of Potentiometric Polymeric Membrane Sensors

Lajos Höfler[1,2], **Iwona Bedlechowicz**[2], **Tamás Vigassy**[2,3], **Róbert E. Gyurcsányi**[1,4,*], **Eric Bakker**[5,*], and **Ernö Pretsch**[2,*]

[1]Department of Inorganic and Analytical Chemistry, Budapest University of Technology and Economics, Szt. Gellért tér 4, H-1111 Budapest, Hungary [2]Institute of Biogeochemistry and Pollutant Dynamics, ETH Zurich, CH-8092 Zurich, Switzerland [3]Research Group of Technical Analytical Chemistry, Hungarian Academy of Sciences, Szt. Gellért tér 4, H-1111 Budapest, Hungary [4]Metroglas AG, Chalchofenstr. 7b, CH-8910 Affoltern am Albis, Switzerland [5]Nanochemistry Research Institute, Department of Applied Chemistry, Curtin University of Technology, Perth, WA 6845, Australia

Abstract

Ion fluxes across polymeric ion-selective membranes are a decisive parameter dictating the lower detection limit of potentiometric ion sensors. An applied current was earlier proposed to counteract such fluxes and reduce the detection limit to ultra-trace levels. So far, however, the method has not been used in practical situations since the correct current amplitude requires prior knowledge of the sample composition. This paper explores the use of the stir effect to evaluate the optimal current by theory and experiments. It is shown that the traditionally used steady-state model assuming a uniform distribution of ion exchanger in the membrane, fixed with time, violates the electroneutrality condition. A modified steady-state model is introduced that allows for a concentration tilt of the ion exchanger and predicts that a stir effect can indeed be utilized to find the optimal current. Ideally, by choosing the optimal current and very long measurement times, the thermodynamic detection limit might be obtained. However, in practice the stir effect declines at low concentrations and the conditions are far from steady state. Therefore, the improvement of the lower detection limit achievable by galvanostatic control is only about one order of magnitude. A numerical finite-difference approximation is shown to trace the experimental potential responses of silver-selective electrodes well, and to reproduce the stir effect adequately, even for different conditioning protocols. The stir effect is successfully used to improve the detection limit of electrodes with ill-optimized inner solutions, however, significant improvements beyond what is commonly feasible by chemical optimization does not seem to be easily achievable. The results indicate that with conventional membranes the possibility of improving the detection limit by current polarization is much more limited than assumed so far.

During the last decade, polymeric membrane-based ion-selective electrodes (ISEs)[1–4] showed a dramatic improvement in their performance.[5,6] After the discovery that zero-current ion fluxes may bias the results by increasing the primary-ion concentration in the sample near the sensing membrane,[7–9] various means have been designed to reduce such fluxes. They include reducing the diffusion coefficients in the membrane,[10–14] adjusting the composition of the inner solution to the sample,[8,15,16] and decreasing the thickness of the unstirred aqueous layer[17,18] (for overviews, see refs. [10,11,19]). By applying one or several of these approaches,

*To whom correspondence should be addressed. E-mail: E-mail: robertgy@mail.bme.hu, E-mail: bakkere@purdue.edu, E-mail: pretsche@ethz.ch.

massively improved lower detection limits and selectivity behavior have been reported for more than ten different ions.[6]

In one approach, zero-current ion fluxes are compensated by migration of ions in the opposite direction, which is achieved by applying an appropriate external current.[18,20–23] With this technique, spectacular improvements in the lower detection limit have been reported for a Ca-ISE ($10^{-8.9}$ M)[20] and a Pb-ISE ($10^{-11.5}$ M)[18] in transient experiments involving exponential dilutions. A theoretical treatment of steady-state responses in the presence of external currents was based on the phase-boundary potential model and was in good qualitative agreement with the above experimental findings.[21] Despite the enormous promise of the method, due to difficulties in predicting the optimal applied current required in samples of unknown composition, this approach could not be applied to practical measurements.

We offer here a deeper insight into the effect of applied currents on the behavior of ion-selective membranes in view of lowering their detection limit. First, with a steady-state model allowing for changes in the concentration profile of both ionophore and mobile sites we show that, in contrast to earlier model predictions,[21] the possible improvement of the lower detection limit is limited. Unfortunately, steady-state conditions in commonly used PVC membranes are achieved only after many hours. It must be, therefore, expected that the response to a sample depends on the preceding history (including conditioning) of the membrane, which affects the concentration profiles in the membrane at the time of measurement but this is not considered in a steady-state model. A number of numerical methods have been reported in the literature to model the non-steady state behavior of ion-selective membranes.[24,25] Here, the results are interpreted in terms of an extended theoretical model based on the finite-difference method, [26] which takes into account membrane concentration gradients of the ion exchanger as a result of the applied current. The validity of this model is demonstrated by reproducing experiments with different previous history of the membrane and utilizing a stir effect as an additional factor to evaluate the optimal current. It was suggested earlier that ion fluxes can be detected by observing the presence of potential drifts upon changing the stirring rate in the sample.[7,27] This method was originally proposed to evaluate the optimal composition of the inner solution.[27] Very recently, the disappearance of an applied current under steady-state conditions was shown to be very useful in a variation of so-called backside-calibration potentiometry, where a zeroing of transmembrane ion fluxes is performed to gain information on the sample composition.[28] In that work relatively thin supported liquid membranes were used in which a steady state is reached in a matter of a few minutes.[29]

THEORY

The phase-boundary potential, E_{PB}, is given by:

$$E_{PB} = \frac{RT}{z_I F} \ln \frac{k_I c_I}{[I^{z_I}]} \quad (1)$$

where R, T, and F stand for the gas constant, absolute temperature, and Faraday constant, respectively, z_I is the charge number and k_I, a function of the standard free energy of transfer of I^{zI} between sample and ISE membrane; c_I and $[I^{zI}]$ are the boundary concentrations of I^{zI} in the aqueous and organic phases, respectively; these concentrations being used as an approximation of the corresponding ion activities. In the following, it is assumed that I^{zI} in the membrane is strongly complexed by the ionophore, L, and that the concentration of uncomplexed ionophore is constant, i.e., it is present in a large excess relative to the ion-exchanger concentration, R_T, added to the membrane (cf. eq 3). As a consequence, a concentration change in the primary-ion complex, $[IL^{zI}]$is always proportional to that in the

free primary ion in the membrane. With E_I^0 containing all constant terms together with the phase-boundary potential on the inner membrane side, the membrane potential is given by:[30]

$$E_M = E_I^0 + \frac{RT}{z_I F} \ln \frac{c_I}{[IL^{z_I}]_f} \quad (2)$$

with $[IL^{zI}]_f$ denoting the concentration of the primary-ion complex on the front (i.e., sample) side of the membrane.

In the absence of an externally applied current, at steady state, c_I, c_J and $[IL^{zI}]_f$ are defined by the concentrations of the primary and interfering ions in the bulk of the sample and the concentration of the primary-ion complex, $[IL^{zI}]_b$, on the inner side of the membrane. It is assumed that the ion concentration on the inner membrane side is kept constant by using an inner solution of relatively high concentration and sufficient volume.

In the presence of one dominating interfering ion, J^z, of valency z equal to that of the primary ion, a fast equilibrium at the phase boundary relates the concentrations, c_I and $[IL^z]_f$, to each other by:

$$K_{IJ}^{pot} = \frac{c_I}{c_J} \frac{[JL^z]_f}{[IL^z]_f} \quad (3)$$

with k_{IJ}^{pot} as the potentiometric selectivity coefficient. From the preservation of electroneutrality in the membrane, $[JL^z]_f = [R^-]_f - [IL^z]_f \times z$, where $[R^-]_f$ is the ion-exchanger concentration at the sample side of the membrane. Inserted into eq 3 results in:[1]

$$\frac{c_I}{c_I + K_{IJ}^{pot} c_J} = \frac{z[IL^z]_f}{[R^-]_f} \quad (4)$$

Corresponding equations are also available for different combinations of mono- and divalent primary and interfering ions where $z_I \neq z_J$.[30] Note that it is here assumed that the sample concentration of interfering ion is sufficiently large, and that its concentration polarization near the membrane is neglected ($c_J = c_{J,bulk}$).

At steady state, the arising zero-current ion fluxes depend on the diffusion coefficients of the ions in both phases and on the thicknesses of the two diffusion layers, i.e., of the membrane (mem) and of the unstirred aqueous layer (aq). With this model, steady-state responses in the presence of ion fluxes have been successfully explained for different cases by calculating c_I and $[IL^{zI}]_f$.[30] This treatment is extended here, in analogy to recent work,[28] to allow for a current-induced concentration gradient of a monovalent ion exchanger in the membrane. This gradient, at steady-state, is a function of the current density, j:

$$\frac{j}{F} = \frac{2D_m}{d_m}(R_T - [R^-]_f) \quad (5)$$

where $[R^-]_f$ in the general case differs from its mean value, R_T, and D_m and d_m are the diffusion coefficient in the membrane (for simplicity supposed to be equal for all diffusing species) and the membrane thickness, respectively. The only mode of ion extraction is assumed to be by

ion exchange between the primary, I^z, and the interfering ion, J^z, resulting in the following charge balance expression at the sample side of the membrane:

$$[R^-]_f = z[IL^z]_f + z[JL^z]_f \tag{6}$$

The concentration of primary-ion complex, $[IL^z]_b$, at the backside of the membrane is described as a function of its mole fraction, x, exchanged at the inner side:

$$[IL^z]_b = x\frac{2R_T^- - [R^-]_f}{z} \tag{7}$$

Note that, in analogy to previous work[28], the value of x is calculated from the composition of the contacting inner solution and the selectivity of the membrane. The relationship between the concentration gradients of the primary ion in the membrane and in the aqueous diffusion layer of the contacting sample is conveniently expressed by:

$$q = \frac{D_m d_{aq}}{D_{aq} d_m} = \frac{c_{I,bulk} - c_I}{[IL^z]_f - [IL^z]_b} \tag{8}$$

where the subscript *aq* denotes the aqueous sample phase. The term $[R^-]_f$ is obtained from solving eq 5 and is inserted into eq 4 and eq 7, which yield two expressions that are combined with eq 8 to eliminate $[IL^z]_f$ and $[IL^z]_b$. This gives an implicit equation that describes c_I as a function of $c_{I,bulk}$:

$$q = \frac{2FD_m(c_I - c_{I,bulk})(c_I + c_J K_{IJ}^{pot})}{d_m xzc_J K_{IJ}^{pot}(j + 2F\frac{D_m}{d_m}R_T) + c_I(j + xzj + 2F\frac{D_m}{d_m}R_T(xz - 1))} \tag{9}$$

Eq 9 is solved with appropriate software for c_I and inserted into eq 2 to describe the phase-boundary potential change. Changes in the primary-ion complex concentration, $[IL^z]_f$, are normally sufficiently small and have no appreciable effect on the observed potential (eq 2), but can be obtained from eq 8 if needed.

In order to describe non-steady-state responses, the time-dependent concentration profiles in the two phases can be calculated with the finite-difference method.[26] Assuming that the diffusion coefficients of the cations, I^{zI} and J^{zJ} are the same (D_C) and that the ion exchanger has an independent diffusion coefficient D_A), we can simulate the diffusion and migration of all mobile ions in the membrane. With this model, the small difference between the neighboring elements is calculated by dividing each phase into N segments of thickness δ. The number of ions, $n_{i,\nu}$, in a segment, ν, after each time step, Δt, is given by:[26]

$$n_{i,\nu}(t + \Delta t) = n_{i,\nu}(t) + \frac{D_i}{\delta^2}(n_{i,\nu-1}(t) + n_{i,\nu+1}(t) - 2n_{i,\nu}(t))\Delta t \tag{10}$$

with t and D_i corresponding to the time step and the diffusion coefficient of the ion i, respectively. For reasons of electroneutrality, the total amount of cations in the membrane is constant so that:

$$\Delta n_{\mathrm{J}} = -\Delta n_{\mathrm{I}} \tag{11}$$

In the segments on both sides of the phase boundary (aq and mem), the concentrations are calculated according to eq 4.

The concentration of interfering ions in the aqueous phase is assumed to be sufficiently high so that it is not significantly altered by the ion exchange across the membrane. Thus, it follows from eq 3 and eq 11:

$$K_{\mathrm{IJ}}^{\mathrm{pot}} = \frac{n_{\mathrm{I}}^{\mathrm{aq}}(t+\Delta t)}{n_{\mathrm{J}}^{\mathrm{aq}}(t+\Delta t)} \frac{n_{\mathrm{J}}^{\mathrm{mem}}(t+\Delta t)}{n_{\mathrm{I}}^{\mathrm{mem}}(t+\Delta t)} = \frac{n_{\mathrm{I}}^{\mathrm{aq}}(t)+\Delta n_{\mathrm{I}}}{n_{\mathrm{J}}^{\mathrm{aq}}(t)} \frac{n_{\mathrm{J}}^{\mathrm{mem}}(t)+\Delta n_{\mathrm{I}}}{n_{\mathrm{I}}^{\mathrm{mem}}(t) - \Delta n_{\mathrm{I}}} \tag{12}$$

and the amount of exchanged primary cations, Δn_{I}, at the interface is given by solving eq 12:

$$\Delta n_{\mathrm{I}} = \frac{1}{2}\left(-n_{\mathrm{I}}^{\mathrm{aq}} - K_{\mathrm{IJ}}^{\mathrm{pot}} n_{\mathrm{J}}^{\mathrm{aq}} - n_{\mathrm{J}}^{\mathrm{mem}} + \sqrt{-4n_{\mathrm{I}}^{\mathrm{aq}} n_{\mathrm{J}}^{\mathrm{mem}} + 4K_{\mathrm{IJ}}^{\mathrm{pot}} n_{\mathrm{J}}^{\mathrm{aq}} n_{\mathrm{I}}^{\mathrm{mem}} + \left(n_{\mathrm{I}}^{\mathrm{aq}} + K_{\mathrm{IJ}}^{\mathrm{pot}} n_{\mathrm{J}}^{\mathrm{aq}} + n_{\mathrm{J}}^{\mathrm{mem}}\right)^2}\right) \tag{13}$$

An applied external current density, j, induces superimposed ion migration fluxes. Assuming the same mobility of the primary and interfering ions (in fact, ion-ionophore complexes) and an independent mobility of the ion exchanger in the membrane, the number of cations, $\mathrm{I}^{z\mathrm{I}}$ and $\mathrm{J}^{z\mathrm{J}}$ transported during the time interval, Δt, from one segment into the next one is given by:[26]

$$\begin{aligned} n_{\mathrm{I},v}(t+\Delta t) = n_{\mathrm{I},v}(t) + \frac{D_{\mathrm{C}}\Delta t}{(D_{\mathrm{A}}+D_{\mathrm{C}})\delta^2 F}\Bigg(&\frac{(n_{\mathrm{I},v}(t)+n_{\mathrm{I},v-1}(t))(\delta j-(D_{\mathrm{A}}-D_{\mathrm{C}})F(n_{\mathrm{I},v}(t)-n_{\mathrm{I},v-1}(t)+n_{\mathrm{J},v}(t)-n_{\mathrm{J},v-1}(t)))}{n_{\mathrm{I},v}(t)+n_{\mathrm{I},v-1}(t)+n_{\mathrm{J},v}(t)+n_{\mathrm{I},v-1}(t)} - \\ &- \frac{(n_{\mathrm{I},v}(t)+n_{\mathrm{I},v+1}(t))(\delta j+(D_{\mathrm{A}}-D_{\mathrm{C}})F(n_{\mathrm{I},v}(t)-n_{\mathrm{I},v+1}(t)+n_{\mathrm{J},v}(t)-n_{\mathrm{J},v+1}(t)))}{n_{\mathrm{I},v}(t)+n_{\mathrm{I},v+1}(t)+n_{\mathrm{J},v}(t)+n_{\mathrm{I},v+1}(t)}\Bigg) \end{aligned} \tag{14}$$

$$\begin{aligned} n_{\mathrm{J},v}(t+\Delta t) = n_{\mathrm{J},v}(t) + \frac{D_{\mathrm{C}}\Delta t}{(D_{\mathrm{A}}+D_{\mathrm{C}})\delta^2 F}\Bigg(&\frac{(n_{\mathrm{J},v}(t)+n_{\mathrm{J},v-1}(t))(\delta j-(D_{\mathrm{A}}-D_{\mathrm{C}})F(n_{\mathrm{I},v}(t)-n_{\mathrm{I},v-1}(t)+n_{\mathrm{J},v}(t)-n_{\mathrm{J},v-1}(t)))}{n_{\mathrm{I},v}(t)+n_{\mathrm{I},v-1}(t)+n_{\mathrm{J},v}(t)+n_{\mathrm{I},v-1}(t)} - \\ &- \frac{(n_{\mathrm{J},v}(t)+n_{\mathrm{J},v+1}(t))(\delta j+(D_{\mathrm{A}}-D_{\mathrm{C}})F(n_{\mathrm{I},v}(t)-n_{\mathrm{I},v+1}(t)+n_{\mathrm{J},v}(t)-n_{\mathrm{J},v+1}(t)))}{n_{\mathrm{I},v}(t)+n_{\mathrm{I},v+1}(t)+n_{\mathrm{J},v}(t)+n_{\mathrm{I},v+1}(t)}\Bigg) \end{aligned} \tag{15}$$

Due to electroneutrality conditions, the number of anions transported is equal to the sum of the transported primary and interfering ions:

$$n_{\mathrm{A},v}(t) = n_{\mathrm{I},v}(t) + n_{\mathrm{J},v}(t) \tag{16}$$

Owing to the high concentration of interfering ions, migration in the aqueous phase can be neglected. Across the phase boundary, the number of cations transported by migration is:

$$\Delta n_{\mathrm{I}} = j\frac{\Delta t}{F}\frac{n_{\mathrm{I,aq}}}{n_{\mathrm{I,aq}} + K_{\mathrm{IJ}}^{\mathrm{pot}} n_{\mathrm{J,aq}}} \tag{17}$$

$$\Delta n_J = j\frac{\Delta t}{F}\frac{K_{IJ}^{pot} n_{J,aq}}{n_{I,aq} + K_{IJ}^{pot} n_{J,aq}} \quad (18)$$

In the presence of an external current, for each time step, first, the contributions by migration are calculated (eq 14, eq 15) and, then, the ion exchange across the phase boundary (eq 13). Finally, the current-induced potential drop ($j \times R_{mem} \times$ (membrane area) 2.54 cm^2) is added to the calculated emf using the membrane resistance from fitting the experimental data (R_{mem} = 0.18 MΩ). The other parameters of the simulations were: $\log K_{AgNH_4}^{pot} = -7.94$, D_{aq} = 1.5×10^{-5} cm^2 s^{-1}, [31] $D_C = 8 \times 10^{-7}$ cm^2 s^{-1}, $D_A = 1.1 \times 10^{-8}$ cm^2 s^{-1},[32] d_{mem} = 330 μm, $d_{aq,stirred}$ = 80 μm, $d_{aq,unstirred} = 10^3$ μm. Two of the parameters, D_C and $d_{aq,stirred}$, were obtained from least-squares fittings to observed time responses. The influence of stirring was assumed to be instantaneous. The thicknesses of the segments in the membrane and in the aqueous phase were chosen as 10 μm each. In earlier calculations, this spatial resolution was found to be sufficient,[26] and several calculations in the present work with ten times thinner segments did not lead to significantly different results.

3. EXPERIMENTAL SECTION

Chemicals

Poly(vinyl chloride), 2-nitrophenyl octyl ether (*o*-NPOE), potassium tetrakis[3,5-bis-(trifluoromethyl)phenyl]borate (KTFPB), and tetrahydrofuran (THF) were purchased from Fluka AG (CH-9471 Buchs, Switzerland). The silver ionophore, (1,3-*alt*-5,11,17,23-tetra-*tert*-butyl-25,27-dipropoxy-26,28-(3,9-dithia-6-oxaundecan-1,11-diyloxy)thiacalix[4]arene, was synthesized according to the published procedure.[33] Solutions were prepared with deionized water (specific resistance, >18 MΩ cm) obtained with a NANOpure reagent-grade water system (Barnstead, 4009 Basel, Switzerland).

Membranes

The membranes consisted of silver ionophore (1.00 wt%, 10.0 mmol kg^{-1}), KTFPB (0.44 wt %, 5.0 mmol kg^{-1}), PVC (43.0 wt%), and *o*-NPOE (55.6 wt%). These components were dissolved in THF and poured into a glass ring (φ 37 mm) fixed on a glass plate. After overnight evaporation of THF, a disk of 25 mm in diameter was punched from the membrane.

Emf Measurements

Measurements were carried out in a symmetric Teflon-plexiglass cell. The two compartments, each containing 50 mL of solution, were separated by the Ag^+-selective membrane (thickness, calculated from the disk weight, 330 μm; diameter in contact with the solutions, 18 mm). Each compartment contained a double-junction reference electrode (type 6.0729.100, Metrohm AG, CH-9101 Herisau, Switzerland).

Potentials were monitored and currents were applied by a μAutolab Type II potentiostat/galvanostat. The galvanic cell was Ag/AgCl/3 M KCl/1 M NH_4NO_3/sample solution//ISE membrane//IFS/1 M NH_4NO_3/3 M KCl/AgCl/Ag.

Two different inner filling solutions (IFS) were used in the inner compartment: IFS1 consisted of 10^{-4} M $AgNO_3$ with 10^{-4} M NH_4NO_3 as background, and IFS2 was 10^{-3} M KBr. Based on the potentiometric selectivity coefficient ($\log K_{AgNH_4}^{pot} = -7.94$), with IFS1, the ion exchange on the inner membrane side was calculated to be negligible. On the other hand, with IFS2, the free Ag^+ concentration was kept at 7.7×10^{-10} M. With $\log K_{AgK}^{pot} = -8.70$, here, 0.25% of

Ag^+ was calculated to be replaced by K^+ on the inner membrane side. Before starting the measurements, the membrane was conditioned in 10^{-4} M $AgNO_3$ with 10^{-4} M NH_4NO_3 in both compartments overnight. Note that considering the slightly acidic pH, the complexation of Ag^+ by NH_3 in IFS1 is negligible. For the measurements with inward primary-ion flux, it was conditioned a second night with the same solution in the measurement compartment and IFS2 on the inner side. Measurements were carried out according to the current and stirring programs given in Table 1 and Table 2. The $AgNO_3$ concentration on the sample side was varied at a constant background of 10^{-4} M NH_4NO_3.

Model Calculations

The model was programmed in Python. On a PC with a Core2Duo T7200 processor and 1 GB RAM, 20,000 simulation steps were done during 1 s of CPU time. The time resolution of the calculations shown in the Figures was 0.01 s.

RESULTS AND DISCUSSION

The detection limit of polymeric membrane-based ISEs has been lowered to highly impressive values in recent years, but thermodynamically predicted detection limits are often still orders of magnitude lower than what has practically been achieved. Much of this is attributed to the fact that undesired zero-current ion fluxes can still not be completely eliminated, and the resulting concentration polarization at the membrane surface dictates the detection limit. Of all methods to lower the detection limit, only the use of current polarization has claimed to reach ultra-trace levels down to the picomolar range.[18,21]

The response behavior of polymeric membrane ISEs at the detection limit with and without current polarization has so far been described with so-called fixed-site models, which assume that the ion exchanger remains evenly distributed in the membrane.[21,30,34] At steady state, one may indeed predict that a current exists where the response behavior of the ISE follows the Nicolsky equation (for ions of the same charge), yielding detection limits that are dictated by the thermodynamic ion-exchange selectivity. This was recently predicted by Morf[21] and again confirmed here. For example, an iteratively determined applied current of exactly −1.2703858333 μA for a membrane area of 0.79 cm^2, with $R_T = 0.0050$ mM, $\log K_{IJ}^{pot} = -8.00$, $c_J = 1.00 \times 10^{-5}$ M, $q = 0.0020$, × = 1.000 (see eq 7) and $D_{aq}/d_{aq} = 0.166667$ dm s^{-1} is indeed predicted in Figure 1A to give a detection limit down to 1.00×10^{-15} M. Note however the number of significant figures with which the experimental parameters should be controlled given that only minuscule changes in the current lead to drastic changes in the response.

Surprisingly, the detection limit calculated in Figure 1A is significantly lower than that predicted on the basis of thermodynamic principles (10^{-13} M), raising suspicions about the physical validity of the underlying model. Indeed, the current density used here results in an ion flux that is larer by four orders of magnitude than that of the primary ion alone before any current compensation (0.127 nA in current units). A closer analysis reveals that the role of the applied current is to induce an ion flux of the interfering ion from the sample to the membrane phase so that the concentration of the interference decreases to near-zero at the aqueous side of the phase boundary. Under such optimal conditions, the calculated primary-ion gradients disappear, with the predicted Nernstian response slope to levels apparently below the thermodynamic limit because of the depleted interference levels at the interface. This situation, however attractive it may appear, is unattainable in practice. The inward flux of the interfering ions must result in an inward concentration gradient within the membrane, thereby directly violating the electroneutrality condition because the model assumptions include a uniform distribution of ion exchanger.

Subsequently, a more realistic steady-state model was developed to allow for a concentration gradient of the ion exchanger (see eq 9). Figure 1B shows calculated steady-state chronopotentiometric calibration curves with applied cathodic currents of varying amplitude. The predicted behavior as a function of applied current mimics that of the previously published behavior upon varying the composition of the inner solution.[35] Cathodic currents, for example, will result in an imposed inward cation flux, which might be used to yield optimal detection limits in complete analogy to a chemical optimization of the inner solution. A Nernstian response to very low concentrations seems principally possible if the correct current could be found for each sample. With even larger applied currents, the detection limit was found to decrease to the thermodynamically predicted value (10^{-13} M), where it now indeed leveled off (data not shown). In this paper, we propose to use stirring experiments to evaluate the disappearance of primary-ion fluxes across the Nernstian boundary layer. Recently, such experiments were utilized successfully to evaluate fluxes in ion-selective membranes.[28,36] The thickness of the Nernst diffusion layer changes as the stirring rate in the sample is altered, and this brings about a potential change if the sample phase boundary concentrations do not remain indifferent. This simple approach offers an additional dimension to the measurements and may possibly be used to find the optimal current to be applied. In Figure 1C, the predicted stir effect is shown if the sample concentration is either increased or decreased by 0.2 orders of magnitude. At high concentrations, there is no stir effect because concentration polarization is irrelevant under these conditions. At low concentrations below ca. 10^{-10} M, the stir effect disappears. Based on the steady-state model, it seems that the stir effect may be used to find the optimal current above this limit, which is lower by approximately one order of magnitude than what is possible with chemical optimization alone.[30,34]

Unfortunately, while the steady-state treatment discussed above is a valuable tool to describe the long-term behavior of the system, it is incapable of predicting practical response kinetics under rapidly changing conditions. However, the stir effect might be also useful for practical measurements when a steady state is not reached. This is illustrated by the example in Figure 2, which shows the responses of a Ag^+-selective membrane to the same sample solution of 10^{-7} M $AgNO_3$ with 10^{-4} M NH_4NO_3 as background electrolyte. The main difference between the two traces lies in the direction from which the 10^{-7} M Ag^+ level was reached (i.e., the past history of the ISE membrane) before the measurement series was initiated according to the current and stirring program in Table 1, yielding the results shown in Figure 2. In both cases, the Ag-ISE was conditioned in 10^{-4} M $AgNO_3$ (with 10^{-4} M NH_4NO_3 as for all sample solutions) overnight. After that, its emf was measured during 10 min according to the current and stirring program in Table 1 either in 10^{-5} M $AgNO_3$ followed by 10^{-6} M $AgNO_3$ as pre-stage for the upper-trace experiment in Figure 2 or in 10^{-9} M $AgNO_3$ followed by 10^{-8} M $AgNO_3$ before starting the lower-trace measurements. As shown by the responses in the absence of an external current, the two initial emf values differ by 1.8 mV and opposite drifts are observed when stirring is stopped: The emf increases for the measurement with a past history of successive dilutions (upper trace) and decreases in the opposite case (lower trace). For the measurement series in the former case, the stir effect disappears at an external current of −1 nA (cf. Table 1. A negative current means that cations are migrating from the sample toward the IFS), and the resulting emf is −135.0 mV corresponding to −134.8 mV after correction with the current-induced potential drop through the membrane ($i \times R = +0.18$ mV). For the measurement series with a past history of successive increase in Ag^+ concentration, the stir effect is still negative at +1 nA and slightly positive at +2 nA. With the latter current, the emf reading is −134.2 mV, corresponding to −134.6 mV after correction for the current-induced potential drop. Thus, by applying the proper current, the difference between the two final emf values is only 0.2 mV. The proposed stirring method appears to be promising. Figure 2 also demonstrates that the finite-difference model is capable of treating such non-steady-state responses.

The model was also used to predict the concentration profiles of the Ag^+ complex and the mobile anionic sites in the membrane at the time when the stir effect disappears (Figure 3). It is apparent that the opposite sign of the emf drift upon stopping the stirring in the absence of an external current is caused by the different concentration profiles of the primary-ion complex in the membrane. Note that minute deviations in the primary-ion concentration on the order of 1 ppm within the outmost membrane layer of 10 μm at the sample-contacting interface lead to differences in the emf values and in the sign of the stir effect. The concentration profile is less steep for the measurement series with decreasing Ag^+ concentrations. This explains why in Figure 2 the initial emf value without external current is well described by the steady-state model for the upper trace but not for the lower one after increasing Ag^+ concentrations.

Experiments with a Ag^+-selective membrane are in good agreement with these predictions. The corresponding current and stirring programs are given in Table 2. Using IFS1 as inner solution, which induces only a negligible ion exchange on the inner side of the membrane, the calibration curves with and without optimized external current are shown in Figure 4A. Without applying a current, the experimental lower detection limit is $10^{-8.1}$ M Ag^+. This is higher than expected in the absence of ion fluxes ($K^{pot}_{AgNH_4} \times a_{NH_4} = 10^{-11.9}$M) but exactly agrees with the value expected owing to zero-current ion fluxes (cf. eq 15 in ref [30]). The topmost calibration curve was obtained with the current optimized at each concentration step on the basis of the stir effect. In this case, the lower detection limit is improved, albeit only by 0.2 logarithmic units, to $10^{-8.3}$ M Ag^+. The calculated curves were obtained with the finite-difference model. Measurements with IFS2, which generates an inward flux of primary ions, are shown in Figure 4B. Evidently, the large super-Nernstian response in the absence of current compensation was strongly reduced but not entirely eliminated. With the optimal current, the emf differences from 10^{-6} to 10^{-7} M Ag^+ and from 10^{-7} to 10^{-8} M Ag^+ are 91.2 and 73.6 mV, respectively.

The improvements obtained in the lower detection limit are much less pronounced than expected on the basis of the steady-state model (Figure 1B). This is apparently a consequence of the non-steady-state situation during the measurements. To analyze the influence of the measuring times, the results of a series of finite-difference calculations are shown in Figure 5A. In all cases, before each measurement at the concentration shown, the membrane was conditioned in a solution of 10^{-4} M Ag^+ and 10^{-4} M NH_4^+ on both sides until reaching steady-state. Then, the optimal current (i.e., the current at which the stir effect disappears) was applied for 5 min, 60 min, or infinitely long. It is apparent that the achievable lower detection limit is significantly worse at short times than at steady state. In Figure 5B, the zero-current ion flux of Ag^+ from the membrane into the sample (calculated in current units) is shown together with the optimal external current for each Ag^+ concentration. It is apparent that much larger external currents than the zero-current value are required to compensate for ion fluxes (note the logarithmic scale of the y axis). As also evidenced in Figure 1B, concentrations below ca. 10^{-9} M become measurable only by inducing a strong ion flux from the sample solution in direction of the membrane. This results in an ever increasing inward flux of interfering ions with increasing current density in cases where the concentration polarization of the primary ion is perfectly compensated.

The numerical results suggest that stir effects may be used to find optimal currents to be applied, but that the detection limit of an electrode already properly optimized chemically cannot be significantly improved galvanostatically. These results may seem to question the significance of a recent report by Peshkova et al.,[23] who found that an iteratively applied current yielded a 10^{-10} M detection limit for a calcium selective electrode. Note, however, that an earlier chemical optimization of similarly formulated calcium selective membranes[37] gave detection limits comparable to that obtained with galvanostatic control, which is compatible with the results found here.

CONCLUSIONS

We proposed here a non-steady-state model to predict the potential behavior of polymer membrane ion-selective electrodes under both zero current and current-polarized conditions. The model fully accounts for conditioning effects, i.e., the previous history of the membrane, which is shown to influence, to a great extent, the potential response at low sample concentrations. The main motivation of the study was to determine the optimal current that can compensate zero ion fluxes (in order to improve the detection limit) by using the experimentally determined potential drifts upon changing the stirring rate in the sample. While the approach has proved to be successful for silver-selective membranes, it is difficult to exactly and reliably compensate ion fluxes through an external current with commonly used membrane geometries. This is mainly due to the interdependence of the current- and concentration-driven ion fluxes, i.e., the applied current influences, in a timely fashion, the ionic composition of the membrane at the sample interface and increases the zero-current ion fluxes to be compensated. The present manuscript demonstrates for the first time that in contrast to promises based on the earlier findings, a significant improvement of the detection limit by external current cannot be robustly achieved for practical purposes with membranes containing mobile ion-exchangers. Better results are expected with thinner membranes and/or enhanced convective transport in the solution, but even in such ideal cases an improvement of more than one order of magnitude over chemically optimized systems seems questionable.

ACKNOWLEDGEMENT

The authors are grateful to the National Institutes of Health (R01-EB002189) for financial support and to Dr. D. Wegmann for careful reading of the manuscript. R.E. Gy. gratefully acknowledges the support of the Hungarian Scientific Fund (OTKA NF 69262) and the Bolyai János Fellowship.

References

1. Morf, WE. The Principles of Ion-Selective Electrodes and of Membrane Transport. New York: Elsevier; 1981.
2. Koryta, J.; Stulik, K. Ion-Selective Electrodes. Cambridge, GB: Cambridge University Press; 1983.
3. Bakker E, Bühlmann P, Pretsch E. Chem. Rev 1997;97:3083–3132. [PubMed: 11851486]
4. Bühlmann P, Pretsch E, Bakker E. Chem. Rev 1998;98:1593–1687. [PubMed: 11848943]
5. Bakker E, Pretsch E. Anal. Chem 2002;74:420A–426A. [PubMed: 11811417]
6. Bakker E, Pretsch E. Angew. Chem., Int. Ed. Engl 2007;46:5660–5668. [PubMed: 17457791]
7. Mathison S, Bakker E. Anal. Chem 1998;70:303–309.
8. Sokalski T, Ceresa A, Zwickl T, Pretsch E. J. Am. Chem. Soc 1997;119:11347–11348.
9. Gyurcsányi RE, Pergel E, Nagy R, Kapui I, Lan BTT, Tóth K, Bitter I, Lindner E. Anal. Chem 2001;73:2104–2111. [PubMed: 11354497]
10. Ceresa A, Sokalski T, Pretsch E. J. Electroanal. Chem 2001;501:70–76.
11. Sokalski T, Bedlechowicz I, Maj-Zurawska M, Hulanicki A. Fresenius' J. Anal. Chem 2001;370:367–370. [PubMed: 11495057]
12. Heng LY, Tóth K, Hall EAH. Talanta 2004;63:73–87. [PubMed: 18969405]
13. Sutter J, Radu A, Peper S, Bakker E, Pretsch E. Anal. Chim. Acta 2004;523:53–59.
14. Chumbimuni-Torres KY, Rubinova N, Radu A, Kubota LT, Bakker E. Anal. Chem 2006;78:1318–1322. [PubMed: 16478128]
15. Qin W, Zwickl T, Pretsch E. Anal. Chem 2000;72:3236–3240. [PubMed: 10939393]
16. Szigeti Z, Malon A, Vigassy T, Csokai V, Grün A, Wygladacz K, Ye N, Xu C, Chebny VJ, Bitter I, Rathore R, Bakker E, Pretsch E. Anal. Chim. Acta 2006;572:1–10. [PubMed: 17723454]
17. Vigassy T, Gyurcsányi RE, Pretsch E. Electroanalysis 2003;15:1270–1275.
18. Pergel E, Gyurcsányi RE, Tóth K, Lindner E. Anal. Chem 2001;73:4249–4253. [PubMed: 11569816]

19. Szigeti Z, Vigassy T, Bakker E, Pretsch E. Electroanalysis 2006;18:1254–1265.
20. Lindner E, Gyurcsányi RE, Buck RP. Electroanalysis 1999;11:695–702.
21. Morf WE, Badertscher M, Zwickl T, de Rooij NF, Pretsch E. J. Electroanal. Chem 2002;526:19–28.
22. Bedlechowicz I, Sokalski T, Lewenstam A, Maj-Zurawska M. Sens. Actuators B 2005;108:836–839.
23. Peshkova MA, Sokalski T, Mikhelson KN, Lewenstam A. Anal. Chem 2008;80:9181–9187. [PubMed: 19551940]
24. Radu A, Meir AJ, Bakker E. Anal. Chem 2004;76:6402–6409. [PubMed: 15516134]
25. Sokalski T, Lingenfelter P, Lewenstam A. J. Phys. Chem. B 2003;107:2443–2452.
26. Morf WE, Pretsch E, de Rooij NF. J. Electroanal Chem 2007;602:43–54.
27. Radu A, Bakker E. Anal. Chem 2003;75:6922–6937. [PubMed: 14670054]
28. Xu Y, Ngeotae W, Pretsch E, Bakker E. Anal. Chem 2008;80:7516–7523. [PubMed: 18778039]
29. Malon A, Bakker E, Pretsch E. Anal. Chem 2007;79:632–638. [PubMed: 17222030]
30. Ceresa A, Radu A, Peper S, Bakker E, Pretsch E. Anal. Chem 2002;74:4027–4036. [PubMed: 12199570]
31. Albright JG, Miller DG. J. Phys. Chem 1972;76:1853–1857.
32. Bodor S, Zook JM, Lindner E, Tóth K, Gyurcsányi RE. J. Solid State Electrochem 2009;13:171–179.
33. Csokai V, Bitter I. Supramol. Chem 2004;16:611–619.
34. Ceresa A, Bakker E, Hattendorf B, Günther D, Pretsch E. Anal. Chem 2001;72:343–351. [PubMed: 11199988]
35. Sokalski T, Zwickl T, Bakker E, Pretsch E. Anal. Chem 1999;71:1204–1209.
36. Radu A, Telting-Diaz M, Bakker E. Anal. Chem 2003;75:6922–6931. [PubMed: 14670054]
37. Sokalski T, Ceresa A, Fibbioli M, Zwickl T, Bakker E, Pretsch E. Anal. Chem 1999;71:1210–1214.

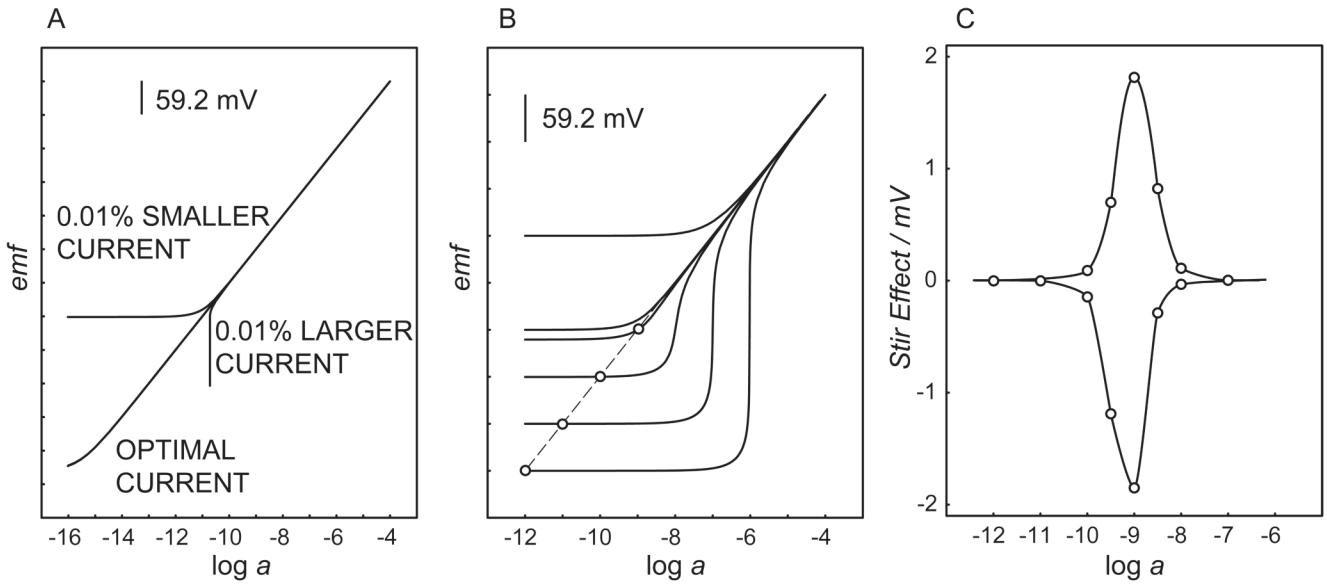

Figure 1.

A) Calculated steady-state calibration curve for a Ag^+-selective membrane with applied currents that are either optimal or deviating by ±0.01%, assuming a fixed, uniform distribution of the ion exchanger in the membrane. See text for parameters used.

B) Steady-state calculations for the same membrane, but allowing for a tilt of ion exchanger in the membrane as a result of the galvanostatic perturbation, and assuming a 1% level of coextraction at the inner membrane side (x = 1.01 in eq 7). Applied currents shown, from top to bottom curves: 0 nA, −6.32 nA, −6.38 nA, −6.96 nA, −12.64 nA, and −66.80 nA, with other parameters as for Figure 1A. The circles denote the optimal Nernstian response for the indicated sample concentration.

C) Calculated steady-state stir effect (potential change upon increasing the thickness of the aqueous diffusion layer by a factor 2), for bulk primary-ion concentrations deviating from the circles in Figure 1B by $\Delta \log c = \pm 0.2$.

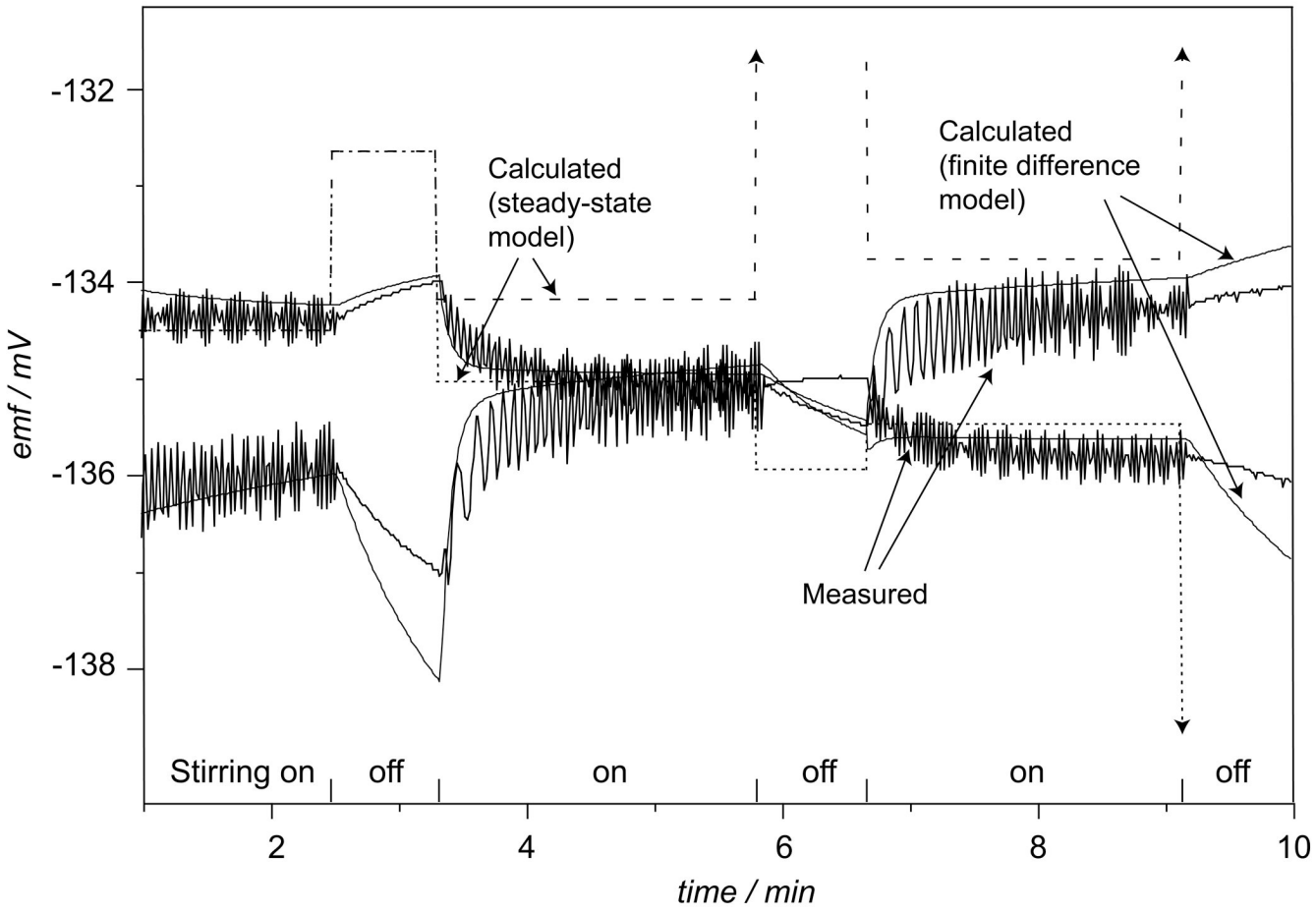

Figure 2.

Time responses of a Ag^+-selective membrane to two identical sample solutions (10^{-7} M $AgNO_3$ with 10^{-4} M NH_4NO_3) observed with different measuring protocols (cf. Table 1): Top: successive dilutions; bottom: successively increasing concentrations. Before both measurements, the membrane was symmetrically conditioned in 10^{-4} M $AgNO_3$ with 10^{-4} M NH_4NO_3 as background electrolyte. Dashed lines are responses predicted by the steady-state model.

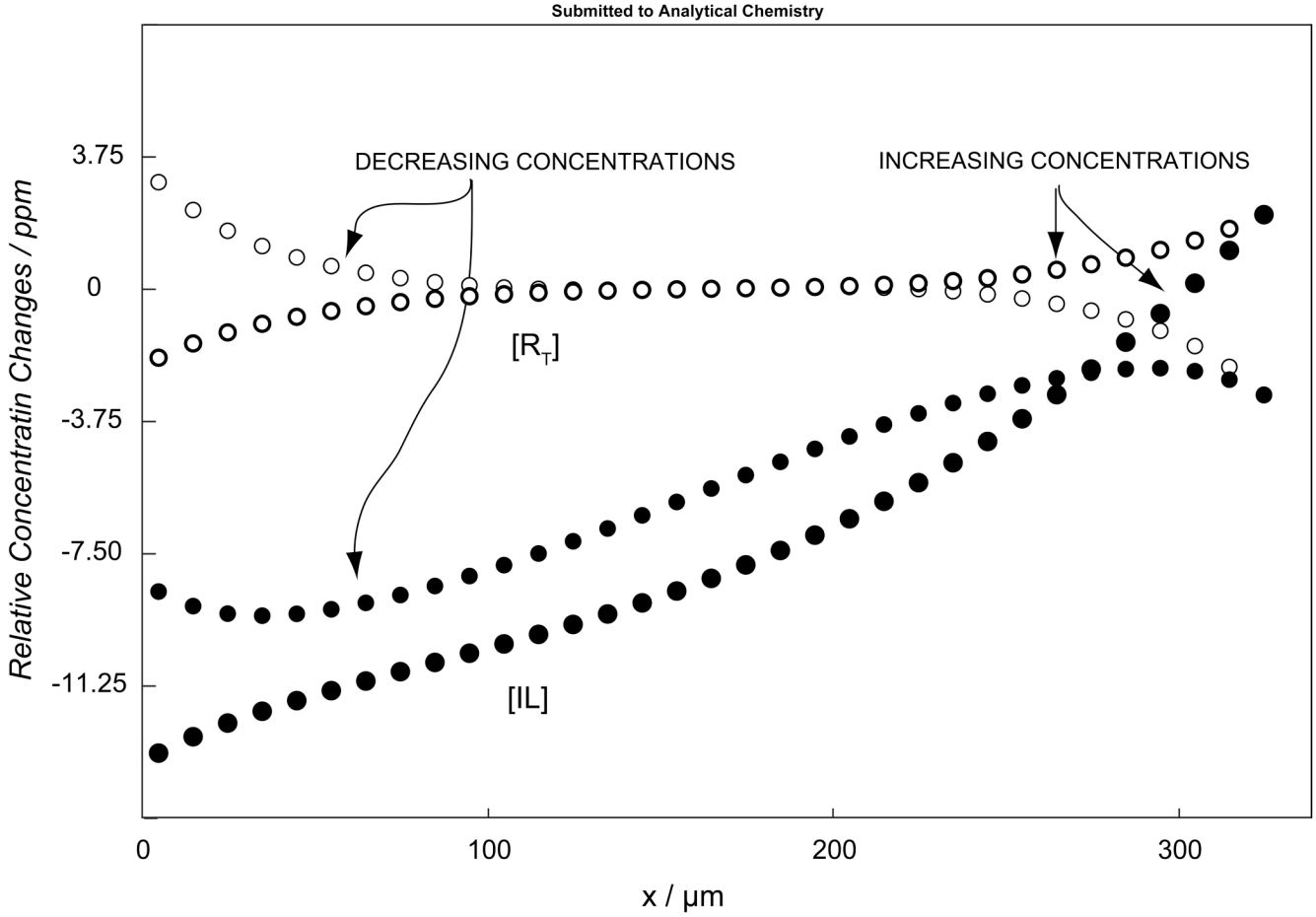

Figure 3.
Calculated concentration profiles in the Ag-ISE membrane at the time when the stir effect in Figure 2 disappears (i.e., at 6 min in the case of previous successive dilutions, and at 9 min when successively having increased the Ag^+ concentrations); x [µm] spatial location in membrane (total membrane thickness, 325 µm).

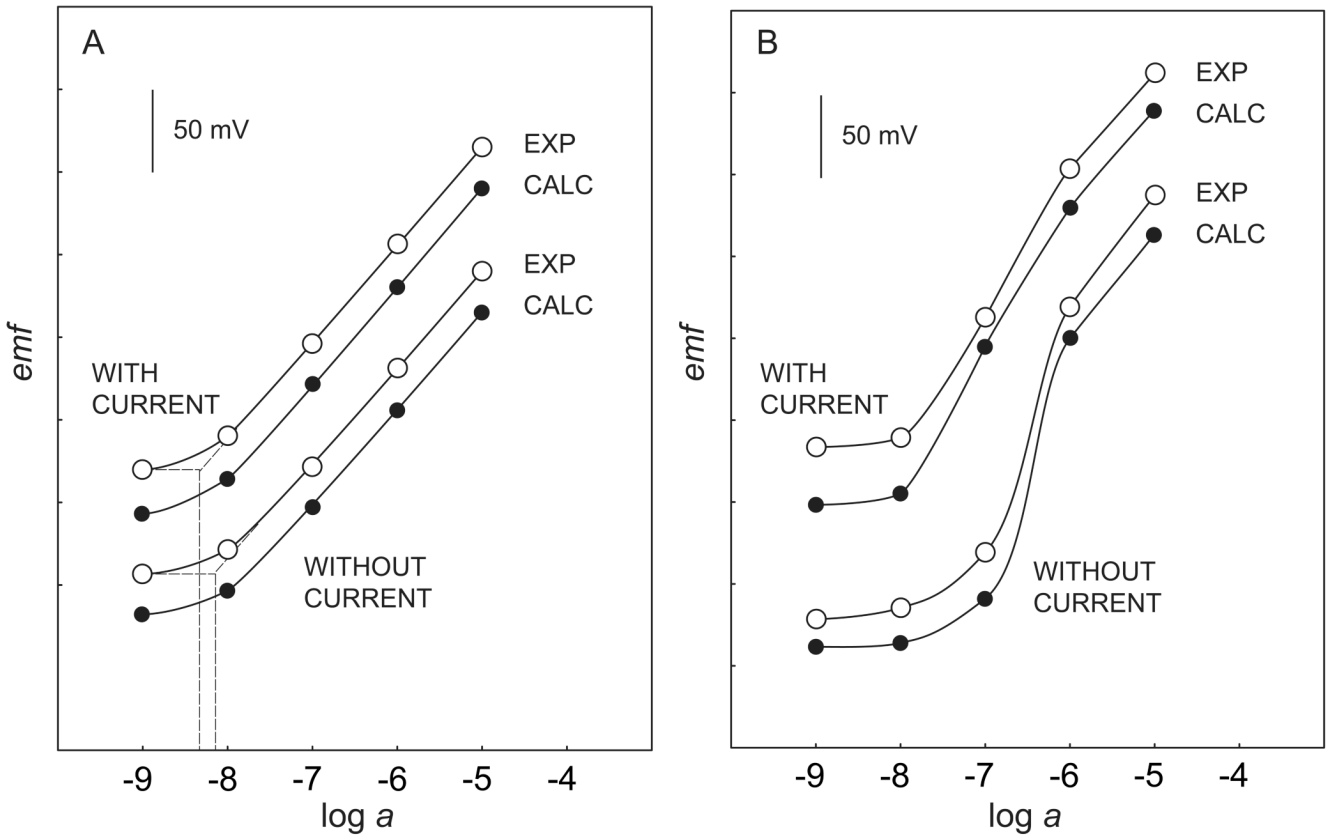

Figure 4.
Calibration curves obtained A) with IFS1; B) with IFS2 (cf. Experimental) with and without current compensation of ion fluxes. In the former case, data were taken at zero stir effect by interpolating the time response curves, and corrected for the $i \times R$ drop.

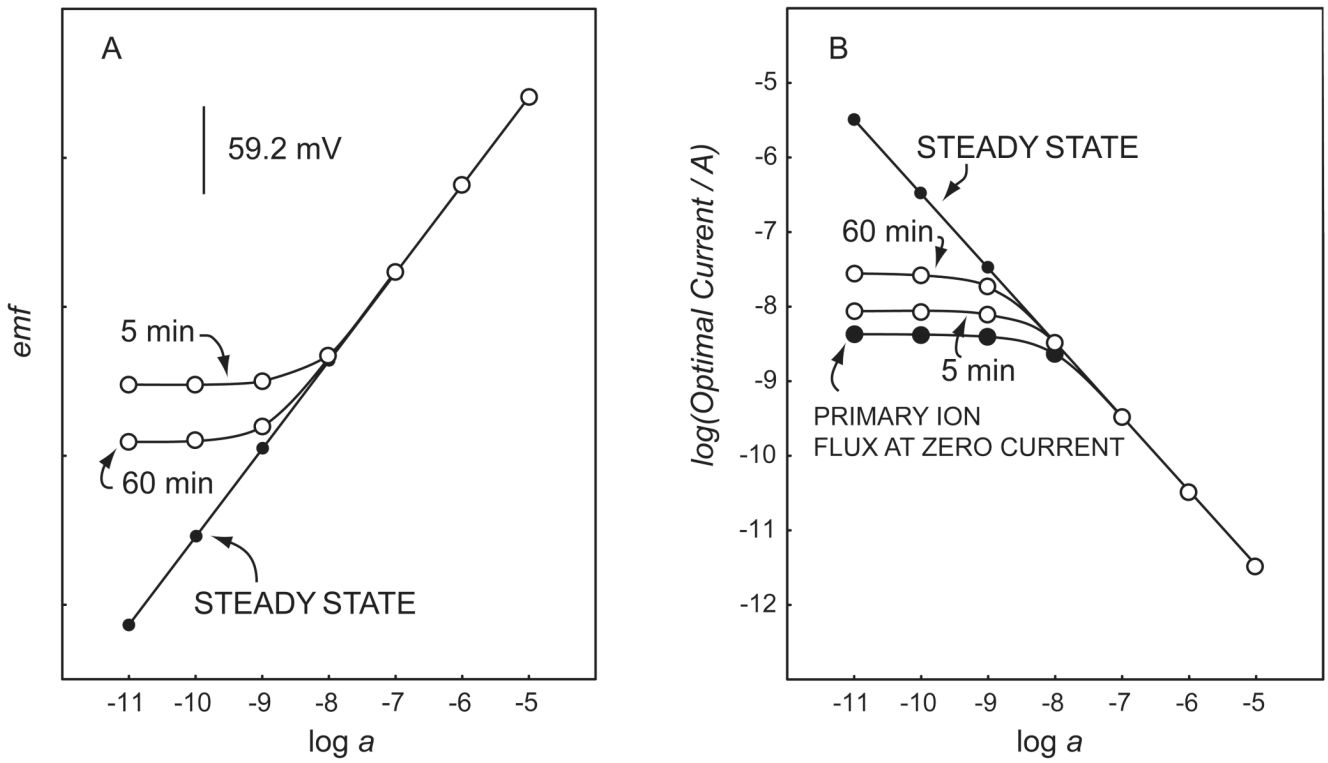

Figure 5.

A) Finite-difference calculations of the responses of a Ag^+-selective electrode with different measuring times. Before each measurement, the membrane was conditioned in a solution of 10^{-4} M Ag^+ and 10^{-4} M NH_4^+ on both sides until steady state and then, the optimal current (i.e., the current at which the stir effect disappears) was applied during the measurement time indicated.

B) Zero-current ion flux of Ag^+ from the membrane into the sample (calculated in current units) and optimal external current for each concentration.

Table 1

Current and Stirring Program for the Experiments Shown in Figure 2 and Figure 3

time / s	stirring	current [nA] for measurements starting at	
		10^{-5} M $AgNO_3$	10^{-9} M $AgNO_3$
0–150	on	0	0
150–200	off	0	0
200–350	on	−1	1
350–400	off	−1	1
400–550	on	−2	2
550–600	off	−2	2

Table 2

Current and Stirring Program for the Experiments Shown in Figure 4

time / s	stirring	current [nA] for Ag-ISE with	
		IFS1 (Figure 4A)	IFS2 (Figure 4B)
0–750	on	0	0
750–800	off	0	0
800–950	on	−1	20
950–1000	off	−1	20
1000–1150	on	−2	50
1150–1200	off	−2	50
1200–1350	on	−5	100
1350–1400	off	−5	100
1400–1550	on	−10	200
1550–1600	off	−10	200
1600–1750	on	−20	500
1750–1800	off	−20	500